High T_c Superconductor-Sapphire Microwave Resonator with Extremely High Q-Values up to 90 K

Zhi-Yuan Shen, *Member, IEEE*, Charles Wilker, Philip Pang, *Member, IEEE*, William L. Holstein, Dean Face, *Member, IEEE*, and Dennis J. Kountz

***Abstract*—A theoretical analysis was performed for an extremely high Q resonator formed by a sapphire rod sandwiched by a pair of high T_c superconductor (HTS) films. A number of these HTS-sapphire-HTS resonators in *C*-band and *Ka*-band were designed, fabricated and tested. At 5.552 GHz, Q_o reached 2×10^6 at 90 K, 3×10^6 at 80 K and 1.4×10^7 at 4.2 K with circulating power up to 500 kW. Formulas for calculating the resonant frequency and Q-value derived from the theoretical analysis were verified by experimental data with good agreement. Three different thin film HTS materials: $Tl_2Ba_2CaCu_2O_8$, $YBa_2Cu_3O_{7-\delta}$ and $Tl_{0.5}Pb_{0.5}Sr_2CaCu_2O_7$ were tested. The sensitivity of the high Q-value and the parasitic coupling to the case modes are discussed. Applications, such as frequency stabilized oscillators, filters and characterization for HTS films are described.**

I. Introduction

THE NEED for frequency stabilized oscillators, low loss filters and slow wave structures drives the search for microwave resonators with ever higher Q-values. Resonant cavities using low T_c superconductors such as niobium and lead achieved extremely high Q [1], [2], but they require liquid helium temperature operation. At higher cryogenic temperatures, sapphire resonators have fairly high Q [3], but they are bulky because of wide spread evanescent fields.

The goal is to design a compact microwave resonator with extremely high Q-value operating at or above liquid nitrogen temperature. A first option might be a hollow cavity with HTS coated on the inner walls. Unfortunately, no high quality (low surface resistance, R_s) HTS materials are available on a curved surface, so that, at least for now, this option is not practical. However, high quality (R_s hundreds times lower than copper) flat HTS films are available, which can be used for confining the electromagnetic (EM) fields with very little loss along at least one direction (say the z-direction in a cylindrical cavity). High purity single crystal sapphire has extremely low loss at liquid nitrogen temperatures. In addition, its relatively high dielectric constant not only helps to reduce the size of the resonator, but also makes the total reflection easier at the interface with air or vacuum. In fact, for the TE_{011} mode in a cylindrical sapphire rod, the EM fields decays almost exponentially along the radial direction away from the surface of the rod. If the radius of the HTS films placed at the end is sufficiently large compared to the radius of the rod, the radial rf leakage is negligible. HTS-sapphire-HTS TE_{011} mode resonators offer the potential for high Q and small size [4]. We have designed, fabricated and tested several HTS-sapphire-HTS TE_{011} mode resonators at 5.552 GHz, 6.480 GHz and 27.33 GHz. In the *C*-band, the unloaded Q-value reaches 2×10^6 at 90 K, 3×10^6 at 80 K and 1.4×10^7 at 4.2 K. The resonator can handle circulating power ranging from 2 kW to 500 kW depending upon the operating temperature. To our knowledge, these represent the highest Q and power handling data published for any HTS microwave device.

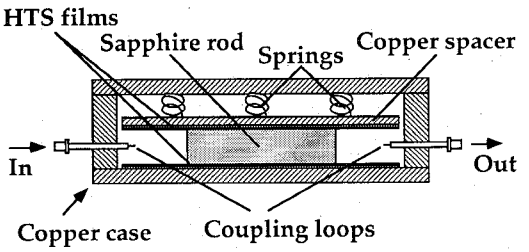

Fig. 1. The configuration of a packaged HTS-sapphire-HTS resonator.

II. Construction of the HTS-Sapphire-HTS Resonator

As shown in Fig. 1, the resonator was formed in a HTS-sapphire-HTS sandwich held in an oxygen-free copper package by an array of beryllium copper springs. The HTS films were $Tl_2Ba_2CaCu_2O_8$ deposited on a 2″ diameter (100) $LaAlO_3$ wafer for the original prototype. Later, $YBa_2Cu_3O_{7-\delta}$ and $Tl_{0.5}Pb_{0.5}Sr_2CaCu_2O_7$ HTS thin films on 2″ wafers were also tested. The dielectric rod was c-axis oriented high-purity single crystal sapphire from Union Carbide. Three different size rods were tested with dimensions: 1.000″ (diameter) × 0.472″ (length), 0.625″ (diameter) × 0.552″ (length) and 0.197″ (diameter) ×

Manuscript received March 31, 1992; revised July 28, 1992. This work is partially supported by the U.S. Department of Commerce Advanced Technology Program, Cooperative Agreement No. 70NANB1H122.

The authors are with E.I. DuPont de Nemours & Company, Inc., Central Research & Development, P.O. Box 80304, Wilmington, DE 19880.

IEEE Log Number 9203714.

0.098″ (length). The magnetic dipole coupling was achieved by a pair of copper coaxial cables with a loop at the end. The coupling can be adjusted by changing the insertion depth of the cables.

III. Theory

The HTS-sapphire-HTS resonator can be treated as a section of circular dielectric waveguide short-circuited by the HTS films at both ends [5], [6]. The TE_{011} mode EM fields between two HTS films can be directly derived from the TE_{01} travelling wave fields in a dielectric waveguide [7]. For simplicity, the losses in the sapphire and HTS films were neglected in the field analysis, the loss effects will be considered as a perturbation. The nonzero field components in a cylindric coordinate (ρ, ϕ, z) system are as follows:

For $\rho \leq a$:

$$E_{\phi 1}(\rho, z) = -jA\frac{2\pi\mu_0 f}{\xi_1} J_1(\xi_1\rho)\sin(\beta z) \tag{1a}$$

$$H_{\rho 1}(\rho, z) = -A\frac{\beta}{\xi_1} J_1(\xi_1\rho)\cos(\beta z) \tag{1b}$$

$$H_{z1}(\rho, z) = AJ_0(\xi_1\rho)\sin(\beta z) \tag{1c}$$

For $\rho \geq a$:

$$E_{\phi 2}(\rho, z) = jB\frac{2\pi\mu_o f}{\xi_2} K_1(\xi_2\rho)\sin(\beta z) \tag{2a}$$

$$H_{\rho 2}(\rho, z) = B\frac{\beta}{\xi_2} K_1(\xi_2\rho)\cos(\beta z) \tag{2b}$$

$$H_{z2}(\rho, z) = BK_0(\xi_2\rho)\sin(\beta z) \tag{2c}$$

where A, B are constants; μ_0 is the magnetic permeability of free space; f is the frequency; $J_n(x)$ $(n = 0, 1)$ is the nth order Bessel function of the first kind; $K_n(x)$ $(n = 0, 1)$ is the nth order modified Bessel function of the second kind; ξ_1 and ξ_2 (both are real quantities) are ρ-direction wave numbers inside and outside of the rod, respectively; β is the z-direction propagation constant. The relation among ξ_1, ξ_2 and β is

$$\beta^2 = k^2\epsilon_r - \xi_1^2 = k^2 + \xi_2^2 \tag{3a}$$

$$k = \frac{2\pi}{\lambda} = \frac{2\pi f}{c} = 2\pi f\sqrt{\epsilon_0\mu_0} \tag{3b}$$

where k, λ, c, and ϵ_0 are the propagation constant, wave length, speed of light, and dielectric constant in free space, respectively. Sapphire is an anisotropic dielectric medium. Even though the transverse dielectric constants are equal, they are different from the longitudinal (c direction) dielectric constant. Fortunately, for all TE modes, $E_z = 0$, and so the dielectric properties of the sapphire rod for TE_{011} mode can be expressed by a single dielectric constant, ϵ_r.

The boundary conditions at $\rho = a$ (a is the radius of the sapphire rod) requires $E_{\phi 1}(a, z) = E_{\phi 2}(a, z)$ and $H_{z1}(a, z) = H_{z2}(a, z)$, according to (1a), (1c), (2a), (2c):

$$\frac{J_1(\xi_1 a)}{\xi_1 a} A + \frac{K_1(\xi_2 a)}{\xi_2 a} B = 0 \tag{4a}$$

$$J_0(\xi_1 a)\, A - K_0(\xi_2 a)\, B = 0 \tag{4b}$$

For A, B having non-trivial solutions, the determinant of (4a), (4b) must be equal to zero, or

$$\frac{J_1(\xi_1 a)K_0(\xi_2 a)}{\xi_1 a} + \frac{K_1(\xi_2 a)J_0(\xi_1 a)}{\xi_2 a} = 0. \tag{3c}$$

The boundary conditions at $z = 0$, and $z = L$ (L is the length of the sapphire rod) require $E_{\phi 1}(\rho, 0) = 0$, $E_{\phi 2}(\rho, 0) = 0$, $E_{\phi 1}(\rho, L) = 0$, $E_{\phi 2}(\rho, L) = 0$. According to (1a) and (2a), for the TE_{011} mode:

$$\beta = \frac{\pi}{L} \tag{3d}$$

Solve the simultaneous (3a)–(3d) for a given set of a, L, ϵ_r, to calculate f, which is the resonant frequency, f_0, for the TE_{011} mode.

The unloaded Q-value, Q_0, of a resonator is defined as

$$\frac{1}{Q_0} = \frac{1}{Q_{0,c}} + \frac{1}{Q_{0,d}} \tag{5a}$$

where $Q_{0,c}$ is the conductor Q; $Q_{0,d}$ is the dielectric Q. In (5a), the radiation loss is neglected since the resonator is enclosed by a metal package. But coupling to case modes is still possible and will be discussed in Section VII. As shown in the Appendix, by using the EM field expressions, the $Q_{0,c}$ and $Q_{0,d}$ for the TE_{011} mode can be expressed as

$$Q_{0,c} = \frac{240\pi^2\epsilon_r}{R_s}\left(\frac{L}{\lambda}\right)^3 \frac{1+R}{1+\epsilon_r R} \tag{5b}$$

$$Q_{0,d} = \frac{1+R}{\tan\delta} \tag{5c}$$

where $\tan\delta$ is the loss tangent of the sapphire. The numerical factor R is the ratio of the electrical energy stored inside to that stored outside the sapphire rod, which is derived in the Appendix as

$$R = \frac{1}{\epsilon_r}\left[\frac{\xi_1 J_0(\xi_1 a)}{\xi_2 K_0(\xi_2 a)}\right]^2 \frac{\int_a^\infty K_1^2(\xi_2\rho)\rho\, d\rho}{\int_0^a J_1^2(\xi_1\rho)\rho\, d\rho}. \tag{5d}$$

Formula (5) can be used for calculating R_s of the HTS films from the measured Q_0.

In order to predict the power handling ability of the resonator, a relationship must be established between the dissipated power, P_0, in the resonator and the maximum

rf magnetic field, H_{max}, or the maximum rf current density, J_{max}, on the HTS films. The rf current on the HTS films located at $z = 0$ and $z = L$ is induced by local rf magnetic field. For the TE_{011} mode, according to (1b), magnetic fields $H_{\rho 1}(\rho, 0)$, $H_{\rho 1}(\rho, L)$ and the corresponding induced current density $J_{\phi 1}(\rho, 0)$, $J_{\phi 1}(\rho, L)$ have a Bessel function, $J_1(\xi_1\rho)$, distribution along ρ direction. $J_1(\xi_1\rho)$ has a maximum value of $J_{1,max} = 0.581865$ at $\xi_1\rho_{max} = 1.84118$. Here ρ_{max} is the radius of a circle where the rf current density reaches the maximum valve, J_{max}. The maximum rf magnetic field, H_{max}, and the corresponding maximum current density, J_{max}, are derived in the Appendix as:

$$H_{max} = J_{1,max}\left\{\frac{2\pi R_s}{P_0}\int_0^a J_1^2(\xi_1\rho)\rho\, d\rho \cdot\left[1 + \epsilon_r R + \frac{240\pi^2\epsilon_r \tan\delta}{R_s}\left(\frac{L}{\lambda}\right)^3\right]\right\}^{-1/2} \quad (6a)$$

$$J_{max} = \frac{J_{1,max}}{\lambda_d}\left\{\frac{2\pi R_s}{P_0}\int_0^a J_1^2(\xi_1\rho)\rho\, d\rho \cdot\left[1 + \epsilon_r R + \frac{240\pi^2\epsilon_r \tan\delta}{R_s}\left(\frac{L}{\lambda}\right)^3\right]\right\}^{-1/2} \quad (6b)$$

where λ_d is the penetration depth.

Circulating power, P_c, is defined as the rf power travelling along the length of the rod and reflected back and forth between the two HTS films to form a resonant standing wave. P_c can be calculated as follows:

$$P_c = \frac{W_0 v_g}{2L} = \frac{Q_0 P_0 v_g}{4\pi L f_0} \quad (7a)$$

$$P_0 = P_{in}(1 - S_{11}^2 - S_{21}^2) \quad (7b)$$

where W_0 is the stored energy in the resonator at $f = f_0$; P_{in} is the incident power measured at the input of the resonator; P_0 is the dissipated power in the resonator at $f = f_0$; v_g is the group velocity for the TE_{01} mode travelling wave in the rod. According to the definition of v_g and (3):

$$v_g = \left[\frac{1}{2\pi}\frac{d\beta}{df}\right]^{-1} = \left[\frac{1}{2\pi}\frac{d}{df}\sqrt{k^2\epsilon_r - \xi_1^2}\right]^{-1} = \frac{c}{\sqrt{\epsilon_r}}\sqrt{1 - \frac{\xi_1^2}{\epsilon_r k^2}} \quad (7c)$$

where c is the speed of light in free space.

IV. Test Setup and Method

The measurements of the HTS-sapphire-HTS resonators were made in a liquid helium storage dewar with a glass epoxy insert. The package is mounted on a copper plate at the end of a stainless steel probe which is evacuated and lowered into the insert. The temperature is controlled over a range of 4 K to 150 K with a pair of 100-W heaters. A HP-8510 vector network analyzer with 1 Hz frequency resolution was used for the measurements. A HP-8449A preamplifier and a Hughes 8030H02F TWT power amplifier with output power up to 30 W were inserted at the input of the resonator for the high power measurements. The loaded Q-value, Q_L, of the resonators was measured with the well known 3-dB band width method.

For a single mode resonator with unequal coupling at its input and output, the relationship between the loaded Q_L and the unloaded Q_0 is as follows:

$$Q_0 = Q_L(1 + \beta_1 + \beta_2) \quad (8a)$$

$$\beta_1 = \frac{1 - S_{11}}{S_{11} + S_{22}} \quad (8b)$$

$$\beta_2 = \frac{1 - S_{22}}{S_{11} + S_{22}} \quad (8c)$$

$$S_{21} = \frac{2\sqrt{\beta_1\beta_2}}{1 + \beta_1 + \beta_2} \quad (8d)$$

where β_1 and β_2 are the coupling coefficients at port-1 and port-2, respectively; S_{11}, S_{22} and S_{21} are the magnitudes of the S-parameters measured at the resonant frequency, $f = f_0$. Formulas (8a), (8b) and (8c) were used to calculate Q_0 from the measured data. Formula (8d) was used for verification. The measurement was repeated three times at each temperature and at each power level. Then port-1 and port-2 were interchanged to repeat the measurement. Most data were collected with relatively strong coupling, S_{21} between 3 dB and 8 dB. However, no severe degradation of Q_0 was observed even with very strong coupling, $S_{21} < 0.2$ dB.

V. Test Data for $Tl_2Ba_2CaCu_2O_8$ Films

$Tl_2Ba_2CaCu_2O_8$ films were used first for the HTS-sapphire-HTS resonator. These low surface resistance $Tl_2Ba_2CaCu_2O_8$ films were deposited on 2-inch diameter (100) $LaAlO_3$ wafer. These films have a T_c of 106 K and surface resistance at 10 GHz as low as 23 $\mu\Omega$ at 4.2 K and 150 $\mu\Omega$ at 77 K. The preparation of the films can be found in ref. [8].

The TE_{011} mode resonant frequency f_0 was calculated from (3). It was verified with the experimental data for three different rod dimensions with resonant frequencies $f_0 = 5.552$ GHz, 6.480 GHz and 27.33 GHz. The discrepancies between theoretical values and experimental data were less than 0.2% with $\epsilon_r = 9.32$.

Fig. 2 shows a typical resonant curve of a HTS-sapphire-HTS resonator with a pair $Tl_2Ba_2CaCu_2O_8$ films operating at 84 K. The loaded Q-value was 2.84×10^6 and the unloaded Q-value was 3.40×10^6.

The circulating power, P_c, was selected to represent the

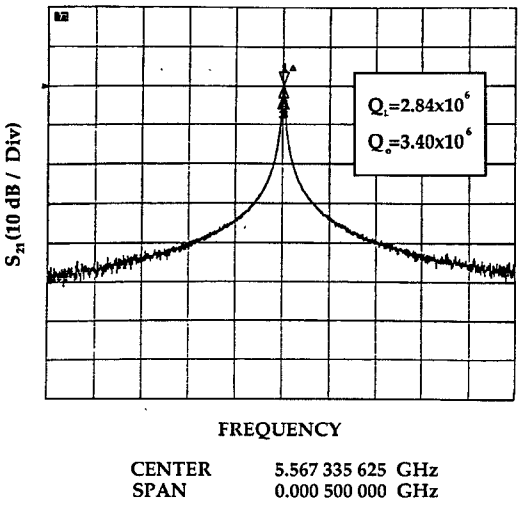

Fig. 2. A typical resonant curve for a *C*-band high Q HTS sapphire-HTS resonator.

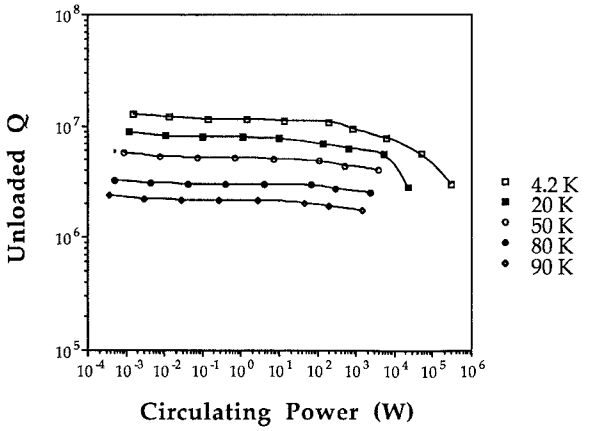

Fig. 3. Unloaded Q-values versus circulating power at different temperatures of a 5.55 GHz $Tl_2Ba_2CaCu_2O_8$ HTS-sapphire-HTS resonator.

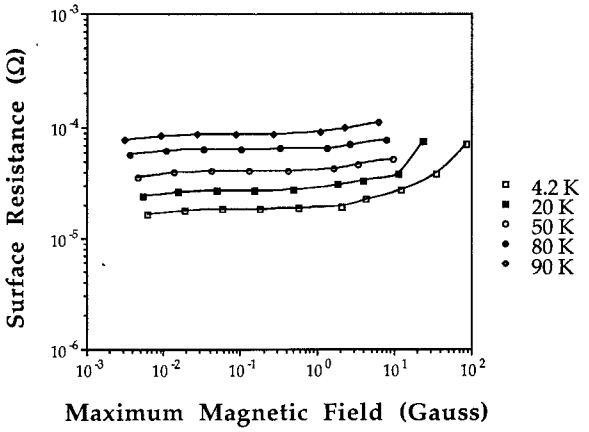

Fig. 4. Surface resistance versus maximum rf magnetic field on the surface of the HTS film measured at different temperatures by a 5.55 GHz $Tl_2Ba_2CaCu_2O_8$ HTS-sapphire-HTS resonator.

power handling of the resonator. Fig. 3 shows the Q_o versus P_c at several different temperatures for a pair of 2″ diameter $Tl_2Ba_2CaCu_2O_8$ films with a 1″ diameter by 0.472″ length sapphire rod.

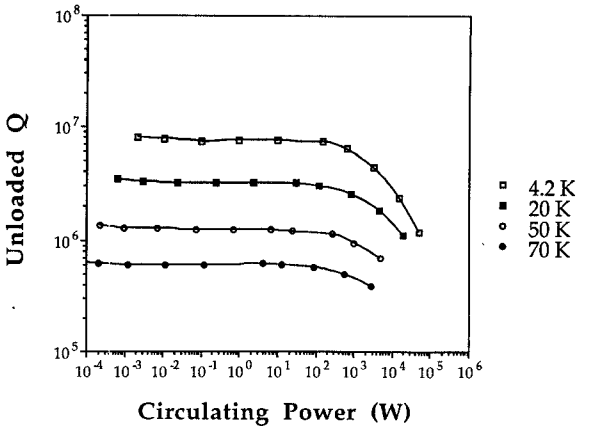

Fig. 5. Unloaded Q-values versus circulating power at different temperatures of a 5.55 GHz $YBa_2Cu_3O_{7-\delta}$ HTS-sapphire-HTS resonator.

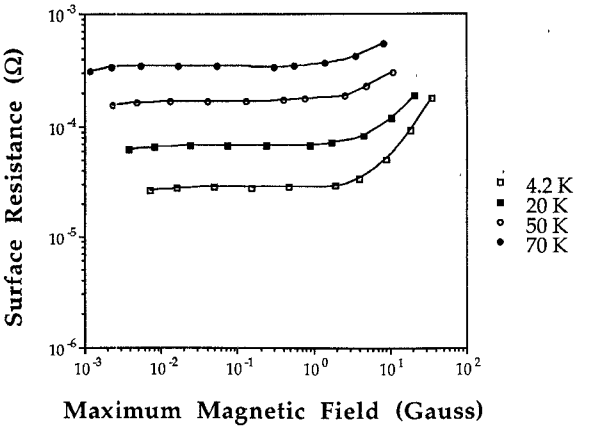

Fig. 6. Surface resistance versus maximum rf magnetic field on the surface of the HTS film measured at different temperatures by a 5.55 GHz $YBa_2Cu_3O_{7-\delta}$ HTS-sapphire-HTS resonator.

Fig. 4 shows the surface resistance, R_s, at 5.552 GHz of a pair of $Tl_2Ba_2CaCu_2O_8$ films as a function of the maximum rf magnetic field, H_{max}.

VI. Test Data for $YBa_2Cu_3O_{7-\delta}$ and $Tl_{0.5}Pb_{0.5}Sr_2CaCu_2O_7$ Films

Tests were also carried out for the 1.000″ × 0.472″ sapphire rod with a pair of 2″ diameter $YBa_2Ca_3O_{7-\delta}$ films and with a pair of 2″ diameter $Tl_{0.5}Pb_{0.5}Sr_2CaCu_2O_7$ films.

The $YBa_2Ca_3O_{7-\delta}$ films were made by co-evaporation of Y, BaF_2 and Cu in an oxygen partial pressure of 1×10^{-5} torr followed by a post-deposition anneal at 850°C for 30 minutes in flowing O_2/H_2O as described in ref. [9]. The film thickness was 3200 Å with a uniformity of better than ±2% over a two-inch wafer.

Fig. 5 shows the Q_0 versus P_c data, Fig. 6 shows the R_s versus H_{max} data for $YBa_2Ca_3O_{7-\delta}$ films at different temperatures.

The $Tl_{0.5}Pb_{0.5}Sr_2CaCu_2O_7$ films were fabricated by first off-axis rf sputtering to produce a precursor film containing lead, strontium, calcium and copper oxides on a (100) $LaAlO_3$ substrate. Films as deposited were nearly stoichiometric and approximately 3500 Å thick. Thal-

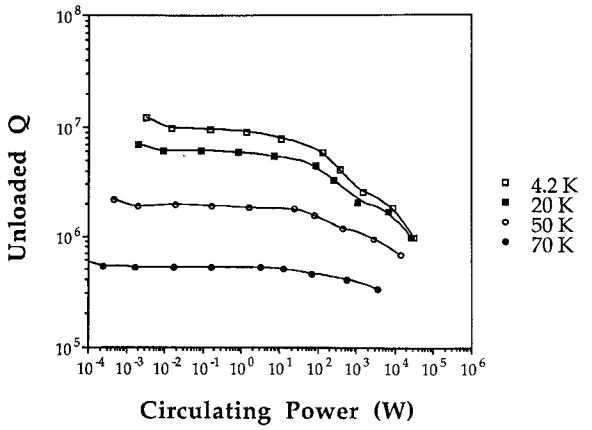

Fig. 7. Unloaded Q-values versus circulating power at different temperatures of a 5.55 GHz $Tl_{0.5}Pb_{0.5}Sr_2CaCu_2O_7$ HTS-sapphire-HTS resonator.

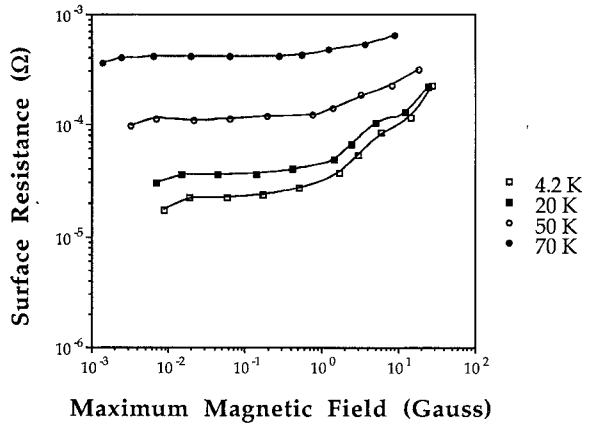

Fig. 8. Surface resistance versus maximum rf magnetic field on the surface of the HTS film measured at different temperatures by a 5.55 GHz $Tl_{0.5}Pb_{0.5}Sr_2CaCu_2O_7$ HTS-sapphire-HTS resonator.

lium was incorporated into the films by a subsequent anneal in the range of 800–900°C for up to 16 hours in a covered alumina crucible containing Tl_2O_3 and $Tl_{0.5}Pb_{0.5}Sr_2CaCu_2O_7$ powder. The details of the process are described in ref. [10].

Fig. 7 shows the Q_0 versus P_c data, Fig. 8 shows the R_s versus H_{max} data for $Tl_{0.5}Pb_{0.5}Sr_2CaCu_2O_7$ films at different temperatures.

Even though the same sapphire rod and the same test setup were used for all three HTS materials, the HTS films used are not necessary the best ones for each particular material. Therefore, any comparison of the performances regarding these HTS materials should be made carefully.

VII. Sensitivity of High Q TE_{011} Mode

Because of its extremely high Q-value, the TE_{011} mode is very sensitive to parasitic coupling to the case modes. Our experience has shown that a -50 dB case mode in the vicinity of the TE_{011} resonant frequency is sufficient to reduce the Q by as much as a factor of three. Special attention must be paid to the design, fabrication and assembly of these high Q resonators.

In the design, two aspect ratios: a/L and b/a (b is the radius of the HTS films), should be carefully selected. In (1) and (2) both $K_0(\xi_2\rho)$ and $K_1(\xi_2\rho)$ are exponential-like decay functions of ρ. A large ξ_2 value means rapid decay, which is favorable for suppressing the parasitic coupling to case modes. The a/L ratio is a main factor in determining the value of ξ_2. By combining (3a), (3b) and (3d), we have:

$$\xi_2 a = \pi\sqrt{\left(\frac{a}{L}\right)^2 - \left(\frac{2a}{\lambda}\right)^2}. \tag{9}$$

Equation (9) can be used for selecting the appropriate a/L ratio under given conditions. For the b/a ratio, theoretically speaking, larger is better. But in reality, b is restricted by the size of the available HTS wafer and a is related to the resonant frequency. The question becomes: What is the minimum acceptable b/a ratio for a specified Q-value? Notice that (1) and (2) are under the assumption that the space outside the rod along ρ-direction is infinite. Otherwise, in the region $\rho > a$ besides $K_0(\xi_2\rho)$ and $K_1(\xi_2\rho)$ terms, there are also $I_0(\xi_2\rho)$ and $I_1(\xi_2\rho)$ terms involved, which represent the reflection of the evanescent fields from the cavity wall and the discontinuity at $\rho = b$. To consider all the details of real boundary conditions, the exact EM field solution is quite complicated. However, an approximate analysis is possible. Define a ratio, ER, which is the electromagnetic energy stored in the "tail" region ($\rho > b$) to the total stored energy in the resonator. As shown in the Appendix:

$$\mathrm{ER} = \frac{1}{2}\frac{\left[1 + \left(\frac{\lambda}{2L}\right)^2\right]\int_b^\infty K_1^2(\xi_2\rho)\rho\, d\rho + \left(\frac{\xi_2\lambda}{2\pi}\right)^2\int_b^\infty K_0^2(\xi_2\rho)\rho\, d\rho}{\epsilon_r\left[\frac{\xi_2 K_0(\xi_2 a)}{\xi_1 J_0(\xi_1 a)}\right]^2\int_0^a J_1^2(\xi_1\rho)\rho\, d\rho + \int_a^\infty K_1^2(\xi_2\rho)\rho\, d\rho} \tag{10}$$

The meaning of the ER value is that if the real HTS wafer radius is b, then this portion of the stored energy will be re-distributed in three ways: 1) some could be absorbed by copper cavity walls; 2) some could be converted into case modes; 3) the rest could be reflected back from cavity walls and still stored in the TE_{011} mode. Since oxygen free copper has fairly low R_s at cryogenic temperatures, the amount for item 1) should be very small. The amount for item 2) depends upon how much the real boundary

condition deviates from the perfect one. The imperfections include gaps, holes, mechanic tolerance of the cavity, the coupling mechanisms, etc. In the worst case (i.e. all the "tail" energy stored in the region $\rho > b$ were to be lost), $1/\mathrm{ER}$ sets the upper limit of the Q_0. In our HTS-sapphire-HTS resonator cases, the ER values were calculated ranging from 10^{-4} to 10^{-5}. The measured Q-values were higher than $1/\mathrm{ER}$, which implies that only a small portion of the "tail" energy is lost. Equation (10) can be used for selecting the b/a ratio.

In the fabrication and assembly of the resonators, tight mechanical tolerances were imposed. Particularly, the c-axis orientation and the parallelism of the end surfaces of the sapphire rod are very crucial. The highest purity single crystal sapphire rods were used. Thorough cleaning procedures were followed. Selective damping was used to suppress any case mode at the vicinity of TE_{011} mode down to less than -60 dB. All these efforts resulted in a repeatable high Q-value upon temperature cycling or after reassembling the resonator.

Because of the extremely high Q, the resonator is sensitive to a microphonic effect. Preliminary observations indicate that most of the microphonic effect is on the amplitude. After the package was redesigned using a much stronger spring, the microphonic effect was drastically reduced. Additional measurements will be performed.

VIII. Applications

One application for the high Q resonator is as the frequency stabilizer for a low phase noise oscillator. Preliminary measurements of an oscillator constructed from an amplifier and a high Q resonator both operating at 80 K indicated that the phase noise was significantly reduced [11]. More accurate phase noise measurements of the oscillator and the resonator are in process.

Another application is to use the high Q resonator as a building block for filters. The use of high Q elements would allow for very low in-band insertion loss, high out-band rejection, steep skirts and extremely high power handling suitable for power transmitters.

Another potential application would be to use the high Q resonator to measure the microwave properties, e.g. surface resistance, R_s, [12], [13] and rf critical current density, J_c, of HTS films. The advantages of this method are: first, it provides an absolute measurement for R_s, no calibration is required; second, it has a very large dynamic range of R_s values; third, it is able to measure the R_s at very high microwave power levels. In fact, due to the extremely high Q, the circulating power inside a moderately coupled resonator is several orders of magnitude higher than the input power. Preliminary data for R_s measured by this method were compared to similar measurements by two other methods (TE_{011} empty cavity end wall replacement [14] and parallel plate [15]) with good agreement. A *Ka*-band HTS-sapphire-HTS resonator for HTS film characterization was built. The low end sensitivity was verified by using a pair of niobium films at liquid helium temperatures. Fig. 9 shows the R_s data of two

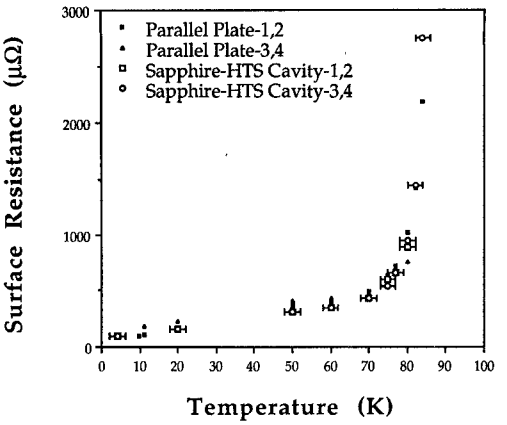

Fig. 9. The surface resistance for two pairs (1,2 and 3,4) of $YBa_2Cu_3O_{7-\delta}$ films measured with a *Ka*-band HTS-sapphire-HTS resonator scaled to 10 GHz assuming f^2 and compared to the data for the same films measured with an *X*-band parallel plate resonator technique.

pairs of 10 mm × 10 mm $YBa_2Ca_3O_{7-\delta}$ films sandwiched with a 0.197″ (diameter) × 0.098″ (length) sapphire rod measured at 27.33 GHz and then scaled to 10 GHz according to a f^2 law and compared to the data of the same film measured with parallel plate method. The coincidence of these data is very good. The details of this method will be published in a separate paper.

IX. Conclusions

In conclusion, extremely high Q-values ($> 10^6$) were obtained from several *C*-band TE_{011} mode HTS-sapphire-HTS resonators at liquid nitrogen temperatures. At liquid helium temperature (4.2 K), the measured Q ($> 10^7$) is comparable to niobium cavities measured at the same temperature [1], [3]. The power handling in terms of circulating power was measured ranging from 2 kW to 500 kW depending upon the operating temperature. The data indicate that $Tl_2Ba_2CaCu_2O_8$, $YBa_2Ca_3O_{7-\delta}$, and $Tl_{0.5}Pb_{0.5}Sr_2CaCu_2O_7$ thin films can be used for high power microwave applications. Theoretical formulas for calculating the resonant frequency and the Q-value were derived and verified by experimental data with good agreement. The sensitivity of the high Q TE_{011} mode and how to suppress the parasitic coupling to case modes were discussed. Several potential applications including low phase noise oscillator, bandpass filter and HTS film characterization were described.

Appendix

Substitute (3d), (4b) into (1), (2). The nonzero field components can be expressed as:

For $\rho \le a$:

$$E_{\phi 1}(\rho, z) = -jA\frac{240\pi^2}{\xi_1 \lambda} J_1(\xi_1 \rho) \sin\left(\frac{\pi}{L} z\right) \quad \text{(A1a)}$$

$$H_{\rho 1}(\rho, z) = -A\frac{\pi}{\xi_1 L} J_1(\xi_1 \rho) \cos\left(\frac{\pi}{L} z\right) \quad \text{(A1b)}$$

$$H_{z1}(\rho, z) = AJ_0(\xi_1 \rho) \sin\left(\frac{\pi}{L} z\right) \quad \text{(A1c)}$$

For $\rho \geq a$:

$$E_{\phi 2}(\rho, z) = jA \frac{240\pi^2}{\zeta_2 \lambda} \frac{J_0(\xi_1 a)}{K_0(\xi_2 a)} K_1(\xi_2 \rho) \sin\left(\frac{\pi}{L} z\right) \tag{A2a}$$

$$H_{\rho 2}(\rho, z) = A \frac{\pi}{\xi_2 L} \frac{J_0(\xi_1 a)}{K_0(\xi_2 a)} K_1(\xi_2 \rho) \cos\left(\frac{\pi}{L} z\right) \tag{A2b}$$

$$H_{z2}(\rho, z) = A \frac{J_0(\xi_1 a)}{K_0(\xi_2 a)} K_0(\xi_2 \rho) \sin\left(\frac{\pi}{L} z\right) \tag{A2c}$$

The conductor Q-value, $Q_{0,c}$, is defined as

$$Q_{0,c} = \frac{2\pi f_0 W_0}{P_{0,c}} \tag{A3a}$$

The dielectric Q-value, $Q_{0,d}$, is defined as

$$Q_{0,d} = \frac{2\pi f_0 W_0}{P_{0,d}} \tag{A3b}$$

Where $P_{0,c}$ and $P_{0,d}$ are the dissipated power in the conductor and in the dielectric at $f = f_0$, respectively.

In a resonant system at $f = f_0$, the total stored energy W_0 is equal to the peak stored electrical energy, which can be expressed as the following:

$$W_0 = W_{e1} + W_{e2} \tag{A4a}$$

where W_{e1} and W_{e2} are the peak electrical energy stored inside ($\rho \leq a$) and outside ($\rho > a$) the sapphire rod at $f = f_0$, respectively. According to field expressions (A1a) and (A2a), W_{e1} and W_{e2} can be calculated as

$$\begin{aligned} W_{e1} &= \frac{\epsilon_0 \epsilon_r}{2} \int_{V_1} E_{\phi 1}^* E_{\phi 1}\, dv = \frac{\epsilon_0 \epsilon_r}{2} \left(\frac{240\pi^2 A}{\xi_1 \lambda}\right)^2 \int_0^{2\pi} d\phi \\ &\quad \cdot \int_0^L \sin^2\left(\frac{\pi}{L} z\right) dz \int_0^a J_1^2(\xi_1 \rho)\, \rho\, d\rho \\ &= \frac{\epsilon_0 \epsilon_r \pi L}{2} \left(\frac{240\pi^2 A}{\xi_1 \lambda}\right)^2 \int_0^a J_1^2(\xi_1 \rho)\, \rho\, d\rho \end{aligned} \tag{A4b}$$

$$\begin{aligned} W_{e2} &= \frac{\epsilon_0}{2} \int_{V_2} E_{\phi 2}^* E_{\phi 2}\, dv = \frac{\epsilon_0}{2} \left(\frac{240\pi^2 A}{\xi_2 \lambda}\right)^2 \left[\frac{\xi_1 J_0(\xi_1 a)}{\xi_2 K_0(\xi_2 a)}\right]^2 \\ &\quad \cdot \int_0^{2\pi} d\phi \int_0^L \sin^2\left(\frac{\pi}{L} z\right) dz \int_a^\infty K_1^2(\xi_2 \rho)\, \rho\, d\rho \\ &= \frac{\epsilon_0 \pi L}{2} \left(\frac{240\pi^2 A}{\xi_1 \lambda}\right)^2 \left[\frac{\xi_1 J_0(\xi_1 a)}{\xi_2 K_0(\xi_2 a)}\right]^2 \int_a^\infty K_1^2(\xi_2 \rho)\, \rho\, d\rho \end{aligned} \tag{A4c}$$

where V_1 and V_2 are the volume inside and outside the rod, respectively. Substitute (A4b) and (A4c) into (A4a):

$$W_0 = \frac{\epsilon_0 \epsilon_r \pi L}{2} \left(\frac{240\pi^2 A}{\xi_1 \lambda}\right)^2 [1 + R] \int_0^a J_1^2(\xi_1 \rho)\, \rho\, d\rho \tag{4d}$$

where $R = W_{e2}/W_{e1}$ is the ratio of electrical energy stored in V_2 to that stored in V_1. The expression for R is given in (5d).

The power dissipated in the conductor, $P_{0,c}$, can be expressed as

$$P_{0,c} = 2 \times \frac{R_s}{2} \left[\int_{S_1} H_{\rho 1}^* H_{\rho 1}\, ds + \int_{S_2} H_{\rho 2}^* H_{\rho 2}\, ds \right]$$

where the factor of 2 is from counting the dissipation in the two HTS films; surface S_1 and S_2 are the film areas covered by the rod ($\rho < a$) and the remaining area ($\rho > a$), respectively. Substitute (A1b), (A2b) into the above equation:

$$\begin{aligned} P_{0,c} &= R_s \left(\frac{\pi A}{\xi_1 L}\right)^2 \left\{ \int_0^{2\pi} d\phi \int_0^a J_1^2(\xi_1 \rho)\, \rho\, d\rho \right. \\ &\quad \left. + \left[\frac{\xi_1 J_0(\xi_1 a)}{\xi_2 K_0(\xi_2 a)}\right]^2 \int_0^{2\pi} d\phi \int_a^\infty K_1^2(\xi_2 \rho)\, \rho\, d\rho \right\} \\ &= 2\pi R_s \left(\frac{\pi A}{\xi_1 L}\right)^2 [1 + \epsilon_r R] \int_0^a J_1^2(\xi_1 \rho)\, \rho\, d\rho \end{aligned} \tag{A5}$$

Substitute (A4d) and (A5) into (A3a). The expression (5b) for $Q_{0,c}$ is proved.

The power dissipated in the dielectric, $P_{0,d}$, can be derived by using the definition of the dielectric loss tangent, $\tan \delta$:

$$\tan \delta = \frac{P_{0,d}}{2\pi f_0 W_{e1}}$$

or

$$P_{0,d} = 2\pi f_0 \tan \delta\, W_{e1} = 2\pi f_0 \tan \delta \frac{W_0}{1 + R} \tag{A6}$$

Substitute (A6) into (A3b), the expression (5c) for $Q_{0,d}$ is proved.

The maximum current density, $J_{\max}$, on the HTS film is related the maximum magnetic field, $H_{\max}$, on the HTS film surface as follows:

$$J_{\max} = \frac{H_{\max}}{\lambda_d} \tag{A7a}$$

where λ_d is the penetration depth. According to (A1b):

$$H_{\max} = \frac{\pi A}{\xi_1 L} J_{1,\max} \tag{A7b}$$

where $J_{1,\max}$ is the first maximum value of Bessel function $J_{1(x)}$. According to (A4b), (A5), (A6), (A7a) and (A7b),

the total dissipated power in the resonator at $f = f_0$ is

$$P_0 = P_{0,c} + P_{0,d} = 2\pi R_s \left(\frac{\pi A}{\xi_1 L}\right)^2 [1 + \epsilon_r R] \cdot \int_0^a J_1^2(\xi_1\rho)\rho\, d\rho + 2\pi f_0 W_{e1} \tan\delta$$

$$= 2\pi R_s \left(\frac{\pi A}{\xi_1 L}\right)^2 [1 + \epsilon_r R] \int_0^a J_1^2(\xi_1\rho)\rho\, d\rho + 2\pi f_0 \tan\delta \frac{\epsilon_0\epsilon_r \pi L}{2} \left(\frac{240\pi^2 A}{\xi_1\lambda}\right)^2 \int_0^a J_1^2(\xi_1\rho)\rho\, d\rho$$

$$= 2\pi R_s \left(\frac{\pi A}{\xi_1 L}\right)^2 \int_0^a J_1^2(\xi_1\rho)\rho\, d\rho \cdot \left[1 + \epsilon_r R + \frac{240\pi^2\epsilon_r \tan\delta}{R_s}\left(\frac{L}{\lambda}\right)^3\right]$$

$$= 2\pi R_s \left(\frac{H_{\max}}{J_{1,\max}}\right)^2 \int_0^a J_1^2(\xi_1\rho)\rho\, d\rho \cdot \left[1 + \epsilon_r R + \frac{240\pi^2\epsilon_r \tan\delta}{R_s}\left(\frac{L}{\lambda}\right)^3\right]. \quad \text{(A7c)}$$

Solve (A7c) for $H_{\max}$, the expression (6a) for $H_{\max}$ is proved, and substitute it into (A7a), the expression (6b) for $J_{\max}$ is proved.

According to the definition of ER:

$$\text{ER} = \frac{1}{2}\frac{1}{W_0}\left\{\frac{\epsilon_0}{2}\int_{V_t} E_{\phi 2}^* E_{\phi 2}\, dv + \frac{\mu_0}{2}\int_{V_t}(H_{\rho 2}^* H_{\rho 2} + H_{z2}^* H_{z2})\, dv\right\} \quad \text{(A8a)}$$

The first numerical factor of $1/2$ on the right side of (A8a) derives from converting the field components from peak values into average values. V_t is the volume of the "tail" region ($\rho > b$). Substitute (A2a), (A2b), (A2c) into (A8a):

$$\text{ER} = \frac{\pi^3\mu_0 L A^2}{W_0 \xi_1^2}\left[\frac{\xi_1 J_0(\xi_1 a)}{\xi_2 K_0(\xi_2 a)}\right]^2 \left\{\left[\left(\frac{1}{\lambda}\right)^2 + \left(\frac{1}{2L}\right)^2\right]\int_b^\infty K_1^2(\xi_2\rho)\rho\, d\rho + \left(\frac{\xi_2}{2\pi}\right)^2 \int_b^\infty K_0^2(\xi_2\rho)\rho\, d\rho\right\}.$$

Substitute (A4d) of W_0 into the above equation, the expression (10) for ER is proved.

Acknowledgment

The authors wish to acknowledge and thank L. A. Parisi for making the $Tl_2Ba_2CaCu_2O_8$ films; R. Small for making the $YBa_2Ca_3O_{7-\delta}$ films; F. M. Pellicone for making the $Tl_{0.5}Pb_{0.5}Sr_2CaCu_2O_7$ films; R. D. Nicholls for surface treatment of the films; M. S. Brenner and C. F. Carter for helping on testing the resonators; Viet Nguyen for the microphonic-resist package design; L. D. Gardenhour and W. Rewa for fabricating the package; and the other members of Du Pont Superconductivity Group for their support.

References

[1] J. P. Turneaure and I. Weissman, "Microwave surface resistance of superconducting niobium," *J. Applied Physics*, vol. 39, 4417–4427, 1968.

[2] H. Hahn, H. J. Halama, and E. H. Foster, "Measurement of the surface resistance of Superconducting Lead at 2.868 GHz," *J. Applied Physics*, vol. 39, 2606–2609, 1968.

[3] D. G. Blair and A. M. Sanson, "High Q tunable sapphire loaded cavity resonator for cryogenic operation," Cryogenics, vol. 29, 1045–1049, 1989.

[4] M. M. Driscoll *et al.*, "Cooled, ultra-high Q, sapphire dielectric resonators for low noise, microwave signal generation," *Proc. 45th Freq. Contr. Symp.*, May 1991, pp. 700–706.

[5] Y. Kobayashi and S. Tanaka, "Resonant modes of a dielectric rod resonator short-circuited at both ends by parallel conducting plates," *IEEE Trans. Microwave Theory Tech.*, pp. 1077–1085, 1980.

[6] Y. Kobayashi, T. Aoki, and Y. Kabe, "Influence of conductor shields on the Q-factors of a TE_0 Dielectric Resonator," *IEEE Trans. Microwave Theory Tech.*, vol. 33, pp. 1361–1366, 1985.

[7] D. Kajfez and P. Guillon, *Dielectric Resonators*, Oxford, MS: Vector Fields, 1990, pp. 75–76.

[8] W. L. Holstein, L. A. Parisi, C. Wilker, and R. B. Flippen, "$Tl_2Ba_2CaCu_2O_8$ films with very low microwave surface resistance up to 95 K," *Appl. Phys. Lett.*, vol. 60, pp. 2014–2016, 1992.

[9] D. B. Laubacher, D. W. Face, R. J. Small, C. Wilker, A. L. Matthews, I. Raistrick, F. H. Garzon, J. G. Berry, P. Merchant, J. Amano, and R. C. Taber, "Processing and yield of $YBa_2Cu_3O_{7-x}$ thin film and devices produced with a BaF_2 process," *IEEE Trans. Magn.*, vol. 27, p. 1418, 1991.

[10] D. J. Kountz, P. L. Gai, W. L. Holstein, C. Wilker, and F. M. Pellicone, "Remarkable microstructural and electronic properties of a highly oriented thin film high temperature superconductor on $LaAlO_3$," presented at *Applied Superconductivity Symp.*, Aug. 20–28, 1992, Chicago.

[11] Z. Y. Shen, P. Pang, C. Wilker, D. Laubacher, W. L. Holstein, and C. Carter, "High Tc superconductor and III-V solid state microwave hybrid circuits," presented at *Applied Superconductivity Symp.*, Aug. 20–28, 1992, Chicago.

[12] S. J. Fiedziuszko and P. D. Heidmann, "Dielectric resonator used as a probe for high T_c superconductor measurements," in *1989 IEEE-MTT-S Int. Microwave Symp. Dig.*, vol. 2, 1989, 555–558.

[13] O. Llopis and J. Graffeuil, "Microwave characterization of high T_c superconductors with a dielectric resonator," *J. Less-Common Metals*, vols. 164 and 165, pp. 1248–1251, 1990.

[14] G. Muller *et al*, "Survey of microwave impedance data of high-T_c superconductors—Evidence for nonpairing charge carriers," *J. Superconductivity*, vol. 3, pp. 235–242, 1990.

[15] R. C. Taber, "A parallel plate resonator technique for microwave loss measurements on superconductors," *Rev. Sci. Instrum.*, vol. 61, pp. 2200–2206, 1990.

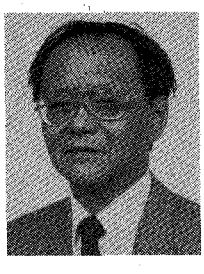

Zhi-Yuan Shen received an advanced degree in radio electronics from Zhejiang University in 1964. He taught there as assistant professor, lecturer, and director of Microwave and Millimeter Wave Laboratories until 1980.

From 1980 to 1983, he was at Polytechnic Institute of new York as visiting scientist doing research on millimeter wave and optical transmission systems. Since 1983, he taught at Bridgeport Engineering Institute as associate professor, and was promoted to full professor at 1984. From 1984

to 1986, he was senior member of technical staff at RLC Electronics, Mt. Kisco, NY. In 1986, he joined Hypres Inc., Elmsford NY, as senior engineer, where he worked on superconducting microwave devices and systems. In 1990, he joined E.I. du Pont de Nemours Company, Wilmington DE, as senior member of technical staff. His current research interest include high T_c superconducting microwave devices.

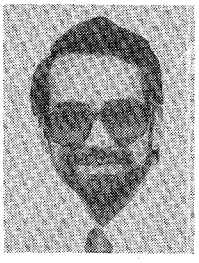

Charles Wilker received the B.A. degree in Physics from Swarthmore College in 1977 and the M.S. and Ph.D. degrees in chemistry from Cornell University in 1979 and 1983, respectively.

In 1984, he joined E.I. du Pont de Nemours & Company where he worked in ceramic electronic materials, and in 1988, he joined the Superconductivity Product Concepts Center. His research interests include the high frequency characterization of high-temperature superconducting films and devices.

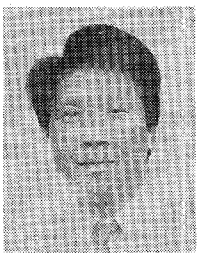

Philip Pang (M'91) received the B.Sc. degree in electronics engineering from the Polytechnic of North London in 1974 and the M.Sc. and PhD. degrees in electronics from the University of Kent in 1975 and 1981, respectively.

From 1981 to 1984, he was with RCL Semiconductor Ltd. working on the research and development of CMOS and NMOS processes. From 1984 to 1990, he was with Litton in the Gould Microwave Product Division working on the research and development of III-V compound semiconductor materials, low-noise devices, power devices, and MMIC design and fabrication. In 1990, he joined E. I. du Pont de Nemours & Company, where he is working on the development of high-temperature superconducting microwave devices.

William L. Holstein received the B.S.E. degree in chemical engineering from Princeton University in 1977 and the M.S. and Ph.D. degrees in Chemical Engineering from Stanford University in 1978 and 1981, respectively. Following a post-doctoral appointment at the Swiss Federal Institute of Technology he joined Du Pont in 1982.

At Du Pont, he has worked in chemical reaction engineering, development of new materials characterization techniques, optical disc technology, optoelectronics, and electronic materials processing. He joined the Superconductivity Product Concepts Center in 1988. His research interests include thin film fabrication and process modeling.

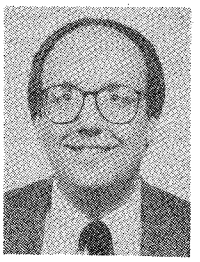

Dean W. Face received the B.S. degree from the California Institute of Technology, Pasadena, CA, in 1979 and the M.S. and Ph.D. in applied physics from Yale University, New Haven, CT, in 1981 and 1986 respectively. His Ph.D. dissertation research was on quantum limited detection and noise in superconducting tunnel junction mixers.

He was a post-doctoral fellow at the Massachusetts Institute of Technology, Cambridge, MA, from 1987 to 1989 where he pursued research on Bi-Sr-Ca-Cu-Oxide thin films and dc SQUID's. He joined the Du Pont Superconductivity group in August, 1989. His research interests include high-temperature superconducting thin films and devices with an emphasis on microwave applications and dc SQUID's.

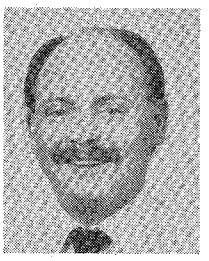

Dennis J. Kountz received the B. A. degree (physics/chemistry) from Wittenberg University, Springfield, OH in 1979. After briefly working for Ashland Chemical Company, Dublin Ohio he received the M.S. and Ph.D. in Physical Chemistry from the Ohio State University, Columbus, Ohio, in 1982 and 1984 respectively. His Ph.D. dissertation research was on the structural characteristics of polydentate phosphorus ligands.

He joined Du Pont in 1984 and developed synthetic fiber technology based on organic polymers and inorganic oxides. In 1988 he joined the Du Pont Superconductivity group where he has developed both bulk and thin film fabrication technology. He is Du Pont's principal investigator for the U. S. Department of Commerce Advanced Technology Program. His research interests include the synthesis and structure versus activity of complex inorganic oxides such as the perovskite-like high-temperature superconducting cuprates.